Water Research 90 (2016) 378–386

Contents lists available at ScienceDirect

Water Research

journal homepage: www.elsevier.com/locate/watres

Toxicity of titanium dioxide nanoparticles on *Pseudomonas putida*

R.G. Combarros, S. Collado, M. Díaz*

Department of Chemical and Environmental Technology, University of Oviedo, Spain

ARTICLE INFO

Article history:
Received 28 October 2015
Received in revised form
22 December 2015
Accepted 23 December 2015
Available online 29 December 2015

Keywords:
Antimicrobial activity
Flow cytometry
Metabolic activity
Pseudomonas putida
TiO_2 nanoparticles
Wastewater treatment

ABSTRACT

The increasing use of engineered nanoparticles (NPs) in industrial and household applications will very likely lead to the release of such materials into the environment. As wastewater treatment plants (WWTPs) are usually the last barrier before the water is discharged into the environment, it is important to understand the effects of these materials in the biotreatment processes, since the results in the literature are usually contradictory. We proposed the use of flow cytometry (FC) technology to obtain conclusive results. Aqueous solutions of TiO_2 nanoparticles (0–2 mg mL^{-1}) were used to check its toxicity effect using *Pseudomonas putida* as simplified model of real sludge over room light. Physiological changes in *P. putida* from viable to viable but non-culturable cells were observed by flow cytometry in presence of TiO_2. The damaged and dead cell concentrations were below 5% in all cases under study. Both FSC and SSC parameter increased with TiO_2 dose dependent manner, indicating nanoparticles uptake by the bacteria. The biological removal of salicylic acid (SA) was also significantly impacted by the presence of TiO_2 in the medium reducing the efficiency. The use of FC allows also to develop and fit segregated kinetic models, giving the impact of TiO_2 nanoparticles in the physiological subpopulations growth and implications for SA removal.

1. Introduction

TiO_2 nanoparticles (TiO_2-NPs) are effective opacifiers profusely used as pigments in paints, paper, inks, and plastics (Li et al., 2014). TiO_2-NPs have chemical stability, high photocatalytic efficiency and low cost (Erdural et al., 2014). Apart from this, TiO_2-NPs have recently become very important as catalyst in photodegradation processes aimed at removing biorecalcitrant and/or toxic pollutants from wastewaters or the inactivation of pathogens in water (Erdural et al., 2014; Ju-Nam and Lead, 2008; Rawat et al., 2007).

Due to this wide application in industries and human daily life, TiO_2-NPs have been detected in soil, surface water, wastewater and sewage sludge samples, which raises concerns about their potential environmental impacts and their possible adverse effects on biological systems (Li et al., 2015, 2014). For instance, TiO_2-NPs were found to adsorb onto activated sludge in conventional biological nutrient removal systems of WWTPs (Li et al., 2015). Nevertheless, the bibliography reports that the factors which might have an impact on interactions between the different types of nanomaterials and biomolecules have remarkably increased, but the knowledge about them is not yet deep (Ghosh et al., 2012; Kumar et al., 2011).

There have been many contradictory reports about the biocompatibility and antimicrobial activity of TiO_2-NPs. Recently, Kapri et al. (2009) and Anil and Zaidi (2010) showed that a bacteria consortium grew faster and to a higher optical density when nanoparticles of nanobarium titanate were added to a bacterial consortium at 0.1 mg mL^{-1}. On the other hand, several researchers indicated a strong antibacterial activity of TiO_2-film on *Escherichia coli* either with irradiate light or sunlight (Bonnefond et al., 2015; Cho et al., 2004; Erdural et al., 2014; Gelover et al., 2006). Erdural et al. (2014) demonstrated that the survival rate of suspended *E. coli* decreased from 100% to 30% in just 60 min, when the bacteria were in contact with TiO_2-film in an irradiated light process; nevertheless, no antibacterial activity was found in the dark process under the same conditions.

The precise mechanism for bacterial toxicity of TiO_2-NP is still being elucidated, but the possibilities include free metal ion toxicity and oxidative stress via generation of reactive oxygen species (ROS) (Besinis et al., 2014; Bonnefond et al., 2015; Cho et al., 2004; Erdural et al., 2014). The cell inactivation has frequently been related to inhibition of cell respiration, decomposition of the lipopolysaccharide layer, DNA damage, genotoxicity, release of toxic constituents and structural disarrangement of the cytoplasmic membrane

* Corresponding author.
E-mail address: mariodiaz@uniovi.es (M. Díaz).

http://dx.doi.org/10.1016/j.watres.2015.12.040
0043-1354/

due to lipid per oxidation (Besinis et al., 2014; Erdural et al., 2014; Ju-Nam and Lead, 2008; Li et al., 2014; Neal, 2008).

Many of these works about effects of TiO_2-NPs on microbial activity almost always based their conclusions on microorganism death, which is usually measured by means of propidium iodide (PI) staining and confocal microscopy (Le et al., 2014), drop-test based on measuring the colony formig unit (CFU mL^{-1}) (Anil and Zaidi, 2010; Bonnefond et al., 2015; Cho et al., 2004; Erdural et al., 2014; Le et al., 2014), or optical density (OD) (Anil and Zaidi, 2010; Besinis et al., 2014). However, after an in-depth bibliographic review, new techniques, such as flow cytometry, which can not only measure the bacterial death but also the reduction in the activity, have not been implemented for this purpose yet. The use of FC provides additional information to the studied so far, where only growth suppression and loss of bacterial viability as CFU mL^{-1} and OD were described (Bonnefond et al., 2015; Cho et al., 2004; Erdural et al., 2014; Fu et al., 2005; Kapri et al., 2009). In addition, most of these researches has been conducted with well-known model organisms, such as *E. coli* (Bonnefond et al., 2015; Cho et al., 2004; Erdural et al., 2014; Fu et al., 2005; Kumar et al., 2011; Rincón and Pulgarin, 2007), with TiO_2-NPs usually forming part of thin film deposit over different surfaces (Bonnefond et al., 2015; Erdural et al., 2014; Gelover et al., 2006).

However, information about their impact on wastewater biological treatments is very scarce (Li et al., 2015, 2014). In fact, as far is known, there are not previous studies dealing with the effect of TiO_2-NPs on *Pseudomonas putida*, even when these bacteria are the predominant ones in activated sludge (Collado et al., 2014) and the results obtained can be employed as a reference during the comparison with those from other works using mixed cultures. Moreover, the use of a pure culture instead of a mixed sludge accelerates and amplifies the response of the system to perturbations (Collado et al., 2014).

Taking into account the aforementioned considerations, the aim of the present work is to evaluate, for first time, the effects of TiO_2-NPs on the viability and activity of *P. putida*. For this purpose, the evolution of the physiological status of *P. putida* when is exposed to different suspended TiO_2-NPs concentrations was studied by means of flow cytometry, distinguishing three metabolic states: viable, damaged and dead cells.

2. Materials and methods

2.1. Preparation of TiO_2 nanoparticle suspension

The TiO_2-NPs used in this study were purchased from Sigma–Aldrich (St. Louis, MO, USA). According manufacturer data, mean nanoparticle size is less than 25 nm, and the purity is 99.5%. Stock solution (50 g L^{-1}) was prepared in sterile Milli-Q water and sonicated (35 kHz frequency, Fisherbrand FB 11010, Germany) for 1 h to disperse the materials (Besinis et al., 2014; Li et al., 2015, 2014; Zucker et al., 2010).

2.2. Cell preparation

P. putida (Leibniz Institute DSMZ-German Collection of Microorganism and Cells Cultures, Germany (DSM 4478)) was chosen. A detailed description of cell preparation procedure can be found in a previous work (Combarros et al., 2014). Stated briefly, *P. putida* colonies were inoculated in a growth medium and incubated at 30 °C and 150 rpm for 16 h. Afterwards, an aliquot was centrifuged and washed at 10,160 × g for 10 min, being then used as an inoculum for subsequent experiments.

2.3. Cell viability test

The effects of TiO_2-NP on the activity and viability of *P. putida* were studied using a synthetic industrial wastewater, composed by a minimum mineral medium which was supplemented by 500 mg L^{-1} of SA, in order to simulate an moderately biodegradable pharmaceutical wastewater. Additionally, some experiments were carried out in the growth medium recommended for *P. putida* by the supplier, with the aim of having a preliminary knowledge about TiO_2-NPs toxicity on *P. putida* under optimal medium conditions. The detailed composition of synthetic industrial wastewater and growth medium can be consulted in Table S1 (see Supplementary data).

For both media, TiO_2-NPs concentrations selected were 0, 0.1, 0.5, 1 and 2 mg mL^{-1}. The stock dispersion diluted with the growth or the simulated industrial medium above at neutral pH, dispersions were sonicated for 1 h prior to assay to ensure dispersion of the particles (Besinis et al., 2014). Typical TiO_2-NPs concentrations reported in bibliography for other toxicity studies usually range from several mg L^{-1} to 1 g L^{-1} (Cho et al., 2004; Le et al., 2014; Li et al., 2015; Rincón and Pulgarin, 2007).

For the growth medium recommended by the supplier (GM), the culture conditions were 200 rpm and 30 °C in 250 mL Erlenmeyer flasks containing 100 mL of simulated medium (Combarros et al., 2014). While, for the simulated industrial wastewater (SIW), the culture conditions were 250 rpm and 30 °C and 100 mL of simulated medium in 500 mL Erlenmeyer flasks (Combarros et al., 2015a). The higher volume and stirring speed selected in the case of SIW were chosen in order to improve the adaptation and growth of bacteria in this medium. In all cases, initial *P. putida* concentration was around 10^7 CFU mL^{-1}. Once *P. putida* was inoculated in the medium, contact TiO_2-NP-bacteria was maintained for 24 h in an incubator New Brunswick Scientific (Edison, New York) that kept constant the culture conditions, taking samples at different times. For each one of them, OD, CFU mL^{-1}, pH, SA concentration and metabolic viability and activity were analysed.

Additionally, experiments with different TiO_2-NP concentrations (0, 0.1, 0.5, 1 and 2 mg mL^{-1}) but without bacteria were also carried out with the aim of discarding possible interactions between TiO_2-NPs and SA.

All material was autoclaved at 121 °C for 20 min in order to maintain the sterility of the system. The TiO_2-NPs and SA stock solutions were sterilized separately.

2.4. Flow cytometry analysis

2.4.1. Staining procedures

The stock solutions preparation and staining procedures have been described in Combarros et al. (2015b). The samples were stained using SYBRgreen (SYBRgreen; Invitrogen) and Fluorescent microspheres (Perfect Count; Cytognos, Spain) to obtain the total count of cells. Additionally, a dual-staining procedure (carboxyfluorescein diacetate/propidium iodide) (cFDA/PI) was used to evaluate the bacterial physiological status: cFDA and PI are indicators of esterase activity and membrane integrity, respectively (Amor et al., 2002; Díaz et al., 2010; Quirós et al., 2007, 2009).

2.4.2. Multi-parameter flow cytometry

Flow cytometry measurements were performed using a Cytomics FC 500 flow cytometer (Beckman Coulter) equipped with a 488 and 633 nm excitation light source from an argon ion laser. Green fluorescence from samples (corresponding to cFDA or SYBRgreen-stained cells) was collected on the FL1 channel (530 nm), whereas PI fluorescence was registered on the FL3

channel (610 nm). Each analysis was performed in duplicate at a low flow rate setting (4000 events s^{-1}). Data acquisition was carried out using Cytomics RXP software (Beckman Coulter). Gates and quadrants were established according to staining controls. For cFDA/PI dual-parameter, data collected from 200,000 events, were analysed using Kaluza® Flow Analysis Software, Beckman Coulter. The fluorescent microspheres presented two types, A microspheres, excitable at 506 nm and B microspheres, excitable between 365 and 650 nm.

2.5. Analytical methods

Concentration of SA in the samples were measured by HPLC (Agilent 1200) using a Mediterranea Sea18 column (5 μm × 25 cm × 46 cm, plus a reverse-phase column from Waters) combined with a UV detector. The wavelength used for detection of SA was 290 nm. The mobile phase consisted in a mixture of two solutions: acetonitrile and 0.4% phosphoric acid in water (Hsu et al., 2004), employing a binary gradient at a constant flow rate of 1 mL min^{-1}.

Number of culturable bacteria (expressed as CFU mL^{-1}) was determined by the standard counting method by plating, obtaining viable counts. The evolution of total biomass was determined by means of two techniques: by optical density measurement at 660 nm (Shimadzu, UV–vis 1203) and by SYBR staining-flow cytometry. In the first case, TiO_2-NPs absorbance was corrected using control samples containing only NPs (Kuang et al., 2013). Viable and total cells were finally expressed in g L^{-1} taking into account the calibration curves previously obtained for viable or total cells stained by SYBRgreen (cell mL^{-1}) versus dry weight (g L^{-1}), respectively.

Physiological status of bacteria were established by means of a multiparameter flow cytometry using a previous dual PI/cFDA staining differentiating metabolically active cells as cFDA stained, dead cells as PI stained and damage cells as PI-cFDA stained. Finally, the cell size and cell complexity were monitored by measuring parameters FSC and SSC respectively by FC.

All experiments were carried out at least in duplicate and each sample was analysed in triplicate. Standard deviations (SD) obtained are shown as vertical lines in figures.

3. Results and discussions

3.1. Antibacterial activity of TiO_2-NPs

Before starting the experiments, it was observed that SA concentration did not change after 24 h in contact with TiO_2-NPs and in absence of *P. putida*, thus precluding any side reactions between TiO_2-NPs and SA (data not shown). Antibacterial test were performed in room light with either growth medium or synthetic wastewater (Fu et al., 2005). Bacterial viability experiments in dark were not carried out since previous studies demonstrate that TiO_2-NPs have no antibacterial effect in dark (Erdural et al., 2014; Fu et al., 2005; Rincón and Pulgarin, 2007). Moreover, Li et al. (2014) discovered that the levels of TiO_2-dependent inhibition of biological nitrogen removal were similar under both dark and light conditions.

3.1.1. Growth medium (GM)

Firstly, in order to get a preliminary estimation of the effect of TiO_2-NPs on the growth and physiological status of *P. putida*, this bacterium has been exposed to different concentrations of nanoparticles in the growth medium recommended by the supplier. Before inoculation, the system TiO_2-NPs-GM was sonicated to ensure de dispersion of nanoparticles. The prepared TiO_2-NPs suspension (0, 0.1, 0.5, 1 or 2 mg mL^{-1}) in GM were inoculated with around 10^7 CFU mL^{-1} of *P. putida* and incubated for 24 h at 200 rpm and 30 °C. In all cases, the initial pH of the media was adjusted to a value of 7.

Fig. 1a shows the evolution of *P. putida* in presence of different concentrations of TiO_2-NPs obtained by means flow cytometry.

The results of total cells obtained by flow cytometry (Fig. 1a) reveal a clear negative effect of TiO_2-NPs on the *P. putida* growth for concentrations higher than 0.5 mg mL^{-1}. Therefore, for TiO_2-NPs lower than 0.5 mg mL^{-1}, *P. putida* showed a fast growth during the first five hours, until forty times the initial bacterial concentration, and then gradually decreases, probably due to the depletion of the GM. However, *P. putida* did not followed this trend for TiO_2-NPs concentrations higher than 0.5 mg mL^{-1}. In such cases, the higher the TiO_2-NPs concentration, the lower the initial *P. putida* growth. Moreover, the final gradual decrease in bacterial population observed for low TiO_2-NPs concentrations after the 5th hour of cultivation is hardly noticeable. Obviously, the lower the bacterial population, the higher the time required for the complete depletion of medium is.

Specific growth rates (μ) for *P. putida* were calculated for every TiO_2-NPs concentrations, getting a value of 0.67 ± 0.01 h^{-1} for TiO_2-NPs concentration equal to or lower than 0.5 mg mL^{-1}, whereas values of 0.501 ± 0.001 and 0.45 ± 0.01 h^{-1} were calculated for 1 and 2 mg mL^{-1} of TiO_2-NPs, respectively. When comparing these results with those reported for *E. coli*, it can be concluded that *P. putida* shows a higher tolerance to TiO_2-NPs than *E. Coli*. Thus, Fu et al. (2005) demonstrated that a 0.40 mg mL^{-1} TiO_2-NPs suspension inhibits effectively the *E. coli* growth.

Fig. 1b shows the FSC and SSC parameters depending on TiO_2-NPs concentration present in the medium. The intensities of FSC and SSC are proportional to the size of cells and the intracellular density, respectively. Although both parameters increased with the TiO_2-NPs concentration, this increase was more marked for SSC than for FSC. So the FSC or SSC signals for the culture with the TiO_2-NPs highest concentration (2 mg mL^{-1}) were around 2 or 13 times higher than those values obtained for cultures without nanoparticles, respectively. Moreover, both parameters are dose-dependent but not time dependent, that is, the increases in their values occur during the first minutes of reaction, then remaining constant (see Fig. S2). Others researches such as Kumar et al. (2011) and Zucker et al. (2010) have observed the SSC increased sequentially while the FSC decreased in response to TiO_2-NPs concentration with *E. Coli* and ARPE-19 cells, respectively, presumably due to substantial light reflection by the TiO_2 particles (Toduka et al., 2012; Zucker et al., 2010).

Several authors reported that the changes in intensity of SSC signal are related to the internationalization of NPs by the bacterium (Ghosh et al., 2012; Kumar et al., 2011). Thus, it seems reasonable to conclude that *P. putida* shows a fast uptake of TiO_2-NPs. Regarding the increase in FSC signal observed, it could be due to the agglomeration of NPs (Ghosh et al., 2012).

3.1.2. Simulated industrial wastewater (SIW)

The effects of different TiO_2-NPs concentrations on the growth and activity of a *P. putida* population are also evaluated, but using in this case a SIW. This wastewater consists of a minimum mineral medium to which 500 mg L^{-1} of SA was added, in order to simulate a moderately biodegradable pharmaceutical wastewater. Fig. 2 shows the evolution on the main parameters under these conditions, such as the bacterial growth or the specific SA removal rates.

Although several studies have been focused on the toxicity of NPs on bacteria, the effect of NPs on their pollutant-degrading activity has hardly been studied. As can be seen in Fig. 2a, the presence of TiO_2-NPs in the SIW involves a reduction in the SA removal

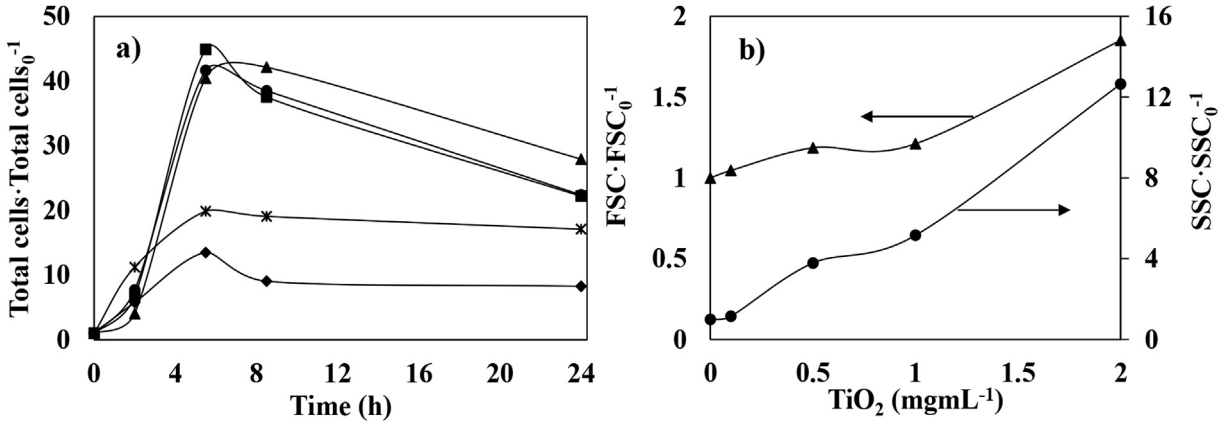

Fig. 1. a) Evolution of total *P. putida* bacteria in GM in presence of different concentrations of suspended TiO_2-NPs: 0 mg mL^{-1} (▲), 0.1 mg mL^{-1} (■), 0.5 mg mL^{-1} (●), 1 mg mL^{-1} (✳), 2 mg mL^{-1} (◆). b) Effect of suspended TiO_2-NPs concentrations on the FSC (▲) and SSC (●) signals after 8 h of *P. putida* cultivation in GM. In all cases: initial SA concentration of 100 mg L^{-1}, 200 rpm, 30 °C, *P. putida* inoculum of 10^7 CFU mL^{-1}, 100 mL in 250 mL Erlenmeyer flasks.

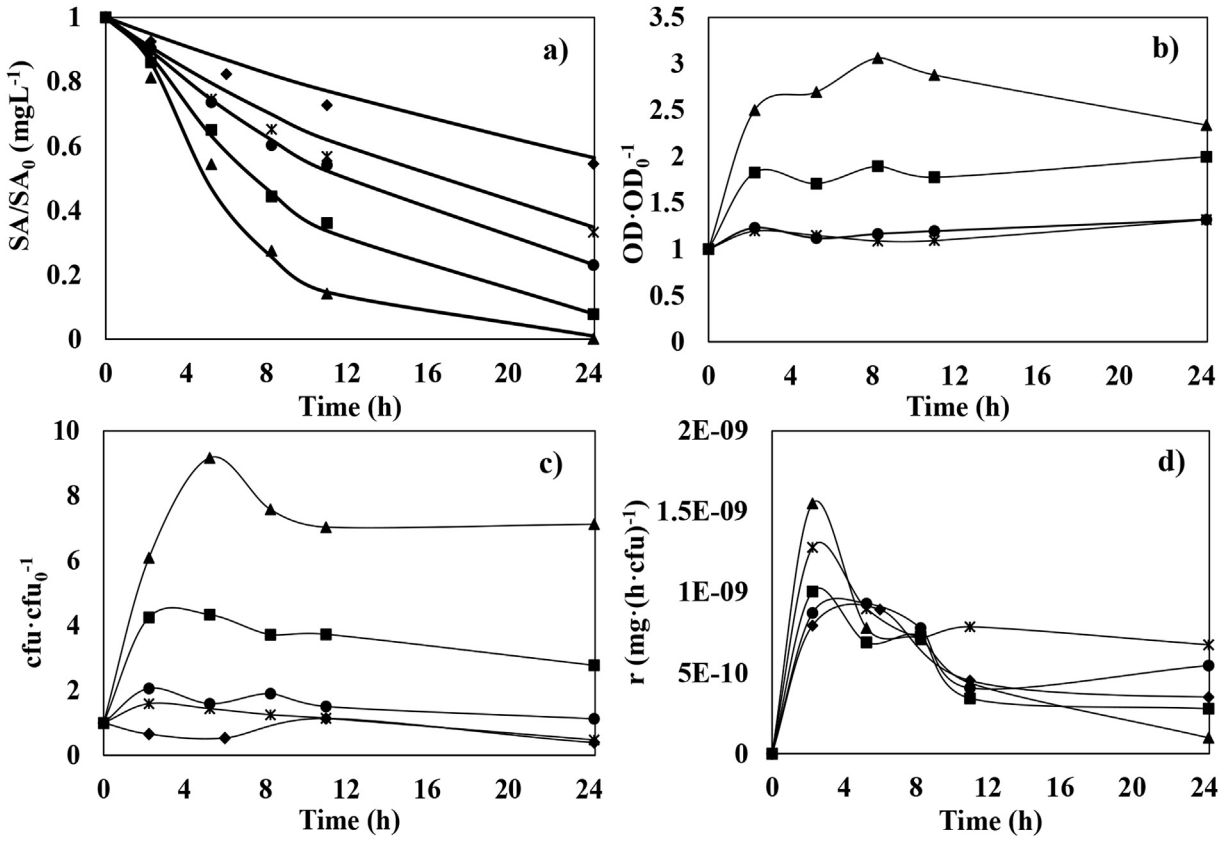

Fig. 2. Evolution of salicylic acid concentration (a), growth of *Pseudomonas putida* as OD (b) or colony forming unit (c) and specific degradation rate of salicylic acid (d) under different TiO_2-NPs concentrations in SIW (▲ 0 mg mL^{-1}, ■ 0.1 mg mL^{-1}, ● 0.5 mg mL^{-1}, ✳ 1 mg mL^{-1}, ◆ 2 mg mL^{-1}). In all cases: Initial SA concentration of 500 mgL^{-1}, 250 rpm, 30 °C, *P. putida* inoculum of 10^7 CFU mL^{-1}, 100 mL in 500 mL Erlenmeyer flasks. Solid lines in Figure a. denote fitting of salicylic acid biodegradation to a pseudo first-order kinetic models.

rate of *P. putida*. For instance, reductions in SA concentration of 86%, 64%, 46%, 43% and 27% were observed after 11 h of cultivation in presence of 0, 0.1, 0.5 1 and 2 mg mL^{-1} of TiO_2-NPs, respectively.

The evolutions of SA concentrations were successfully fitted to a pseudo first reaction order model ($C=C_0 \cdot e^{(-k \cdot t)}$), obtaining the pseudo first order kinetic constant (k) for each TiO_2-NPs concentration. The relation between the k value and TiO_2-NPs concentration in the medium is represented by the following equation:

$$k\left(h^{-1}\right) = 0.20 + 0.040 \cdot TiO_2^{0.49}\left(mg\ mL^{-1}\right)\left(r^2 = 0.95\right)$$

Fig. 2b and c shows the bacterial growth measured as optical density or as colony forming units, respectively. Both parameters followed the same trend, that is, a fast increase in their value during the first hours of cultivation, then remaining approximately constant. It can also been clearly seen in these figures that the presence

of TiO_2-NPs in the SIW reduced the *P. putida* growth, this effect being significant even for low concentrations of nanoparticles. So, the bacterial growth dropped by half with only 0.1 mg mL^{-1} and the growth of the bacteria was almost completely inhibited for TiO_2-NPs concentrations in SIW higher than 0.5 mg mL^{-1}. This trend is better observed when the specific growth rates (μ) are calculated for each concentration of nanoparticles. The μ values obtained from CFU data were 0.41 ($r^2 = 0.82$), 0.26 ($r^2 = 0.70$), 0.08 ($r^2 = 0.99$), 0.07 ($r^2 = 0.85$), and 0.01 ($r^2 = 0.93$) for 0, 0.05, 0.1, 0.25, 0.5 and 1 mg mL^{-1} of TiO_2-NPs, respectively. The relation between the μ value and TiO_2-NPs concentration in the medium can be represented by the following equation:

$$\mu\left(h^{-1}\right) = 0.037 \cdot TiO_2^{-0.93}\left(mg\ mL^{-1}\right)\left(r^2 = 0.87\right)$$

Comparing these results with those previously obtained in GM, it can also be pointed out that, as expected, the inhibitory effect of TiO_2-NPs on the *P. putida* growth is more marked when the availability of carbon or nitrogen is limited. Finally, the specific degradation rates are shown in Fig. 2d; presented a maximum value at around 3 h, this trend was similar with all TiO_2-NPs concentrations.

In regards to flow cytometry measurements in presence of different concentrations of TiO_2-NPs, Fig. 3 plots the evolution of *P. putida* subpopulations, that are, total ($SYBR^+$), viable (as CFU), viable but not culturable (VBNC) ($cFDA^+$ less CFU), active ($cFDA^+$), damaged (PI^+ $cFDA^+$) and dead (PI^+ $cFDA^-$) bacteria. A more detailed description about the gates selected for each subpopulation can be found in SI, Fig. S3. At this point, it is important to point out that a study about the fluorescence emitted by the TiO_2-NPs itself or by its interactions with the dyes used (SYBRgreen, PI, cFDA) was previously carried out (data no shown). Results indicated that the fluorescence emitted by TiO_2-NPs either alone or in presence of fluorochromes, was always lower than 5%, so that, this fluorescence was not considered as significant. Therefore, interferences of TiO_2-NPs with the flow cytometry procedure were discarded.

Results of total cell concentration by flow cytometry are in accordance with those obtained by means of OD and plate counting. So, the presence of small amounts of TiO_2-NPs in the SIW involves a significant reduction in the *P. putida* growth. So, flow cytometry measurements indicated maximum total bacterial populations of $(1.7 \pm 0.4)\cdot 10^8$, $(1.4 \pm 0.1)\cdot 10^8$, $(9.2 \pm 2.8)\cdot 10^7$, $(6.8 \pm 0.2)\cdot 10^7$ and $(3.3 \pm 0.5)\cdot 10^7$ cells mL^{-1} after 3 h of cultivation with 0, 0.1, 0.5, 1 and 2 mg mL^{-1} of TiO_2-NPs, respectively (Fig. 3a). Total bacteria concentrations at zero time for all experiments were around 10^7 cell mL^{-1}. Concentration of *P. putida* subpopulation in percentage and cells mL^{-1} are shown in Fig. 3b–f for 0, 0.1, 0.5, 1 and 2 mg mL^{-1} TiO_2 concentration, respectively. In order to observe better the trends of the subpopulations, the Figs. S4 and S5 show each subpopulation (non-damaged, damaged and dead cells (S4) and actives, viable and VBNC cells (S5)) with time under different TiO_2-NPs concentrations.

The decrease in total cell concentrations observed in Fig. 3a for high times indicates that dead bacteria are rapidly lysed. This trend can be also observed in the evolution of non-damaged subpopulation (PI^-) (see Fig. S4a). So, the higher the TiO_2-NPs concentration, the lower the number of bacteria that have not lost their membrane integrity. However, when non-damaged cells are expressed as a proportion of total cells (see Fig. S4b), it is noteworthy that the higher percentages were obtained for the higher TiO_2-NPs concentrations. These results suggest that a high TiO_2-NPs concentration decreases the number of total *P. putida*, but the surviving bacteria show a better physiological status. In other words, the presence of TiO_2-NPs in the SIW reduces the number of total bacteria but also has an effect of screening, allowing obtaining a final population composed almost entirely for non-damaged bacteria (99% for 2 mg mL^{-1} of TiO_2-NPs in front of 95% in absence of nanoparticles). These results are in accordance with the evolution of damaged and dead subpopulations (Figs. S4c–d and S4e–f, respectively). As can be seen in both figures, either the percentages of dead or damaged cells are lower when the highest concentrations of nanoparticles were used. It can be also pointed out that both subpopulations never exceeded the 5% of the total population, which corroborates the fast lysis of the dead cells observed in Fig. 3a. It is also remarkable that for TiO_2-NPs concentrations lower than 0.1 mg mL^{-1}, the presence of nanoparticles increases the percentage of damaged bacteria, whereas concentrations higher than this value has the opposite effect, that is, the percentage of cells that have lost their membrane integrity decreased. In fact, the proportion of damaged cells in the SIW with 2 mg mL^{-1} of TiO_2-NPs was one order of magnitude lower than in absence of nanoparticles. In the light of these results, it seems reasonable to propose that *P. putida* in presence of TiO_2-NPs concentrations higher than 0.1 mg mL^{-1} are transformed into dead cells, which are rapidly lysed, with a small population of non-damaged bacteria remaining at the end of the experiment. PI cells stained discrimination in *E. coli* exposed to TiO_2 NPs using FC was carried out by Kumar et al. (2011), obtaining values of dead cells between 3.5 and 10% with TiO_2-NPs concentrations of 10–80 $\mu g mL^{-1}$. However, Zucker et al. (2010) observed that TiO_2-NPs showed a minimal decrease in cell viability (2%) in human-derived retinal pigment epithelial cells, at the highest concentration tested (30 $\mu g\ mL^{-1}$), this being measured as PI membrane permeability.

The impact of TiO_2-NPs in activity and culturability of *P. putida* can be seen in Fig. S5a-d. At this point, it is important to emphasize that active *P. putida* were defined as those stained by cFDA, whereas viable cells were measured by plate counting (Quirós et al., 2007, 2009). Again, the higher concentration of nanoparticles, the lower the active or culturable subpopulations. Nevertheless, when the viability results are expressed as percentage of total cells, it should be noted that the lower proportion of viable bacteria were obtained not with 2 mg mL^{-1}, but with concentrations between 0.1 and 0.5 mg mL^{-1}, as in the case of the percentage of damaged cells. This behaviour is not unexpected because both parameters are related to one another: damaged bacteria have lost their membrane integrity and are supposed to be uncapable of showing reproductive growth (Ziglio et al., 2002). The evolution of viable but non-culturable subpopulation, calculated as the active minus the viable subpopulations, also corroborates this assertation (Fig. S5e–f). It should be also noted that nearly all the total population is active but only around one third is culturable when high concentrations of TiO_2-NPs are used. It is well known that plate-culturing techniques only reveal a small proportion of the total microbial population (Giraffa, 2004) For instance, several authors have reported that it was only possible to recover 5–15% of the total bacteria in sludge, regardless the optimization of the cultural medium (Hammes et al., 2008; Ziglio et al., 2002). Finally, it was also observed that the addition of increasing amounts of TiO_2-NPs did not really correspond to an increased in cell death rate but accelerated the transition to VBNC states. SA was consumed in all assays, showing the metabolic activity associated with the VBNC state. As it was previously observed (Quirós et al., 2007, 2009), VBNC maintain the transport and biosynthesis systems, and are able to metabolize substrates. In our experiments, the cFDA fluorescence intensity was maintained during overall bacterial growth, so it can be considered that bacterial VBNC cells were able to preserve the whole enzymatic activity (Quirós et al., 2007). This can be clearer observed in Supplementary material, Fig. S6, where the SA removal rate per cell is represented. Therefore, the similar specific rates observed for all the TiO_2-NPs concentrations confirms that each non-dead

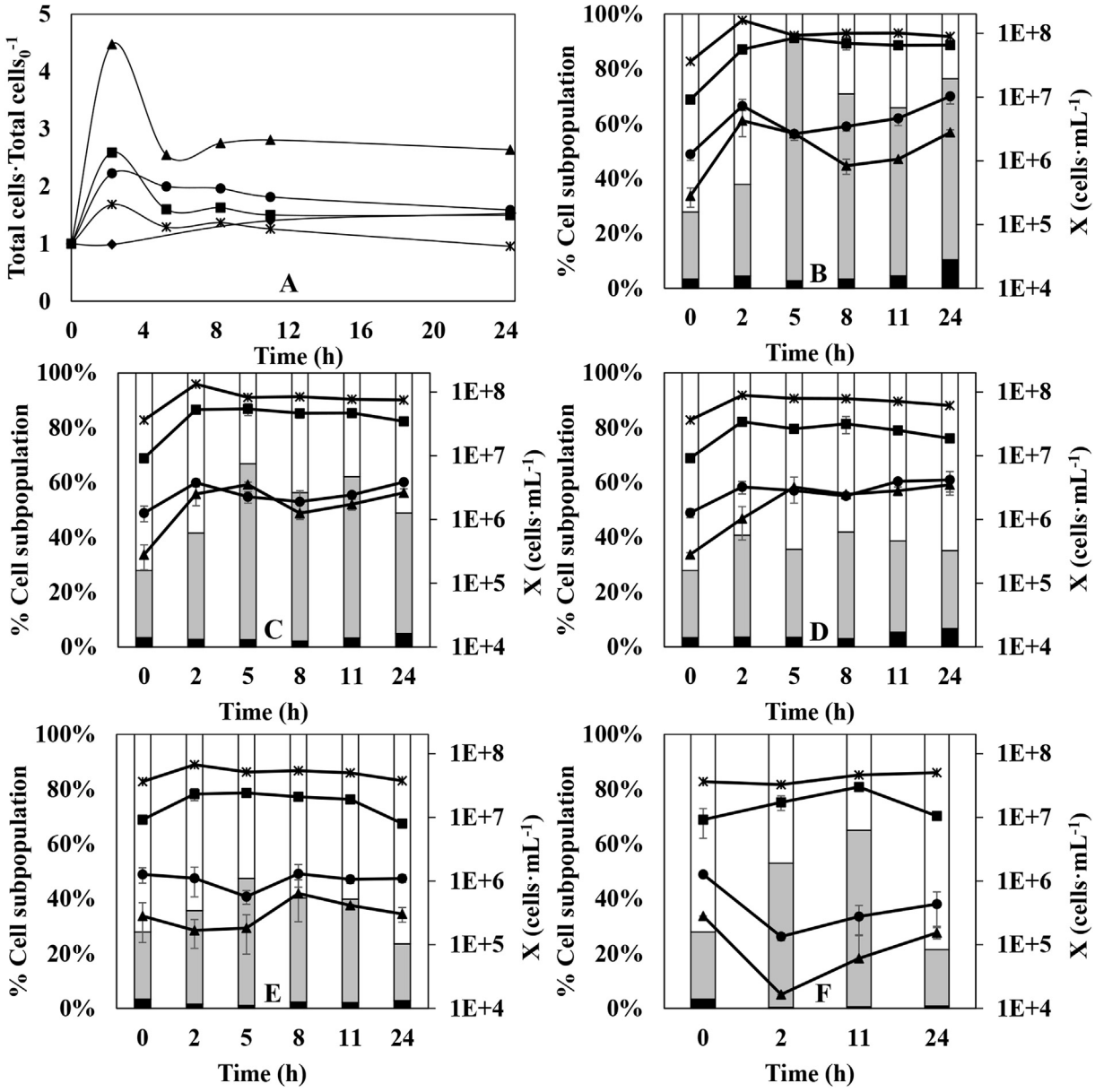

Fig. 3. Total cells concentration (A) (▲ 0 mg mL^{-1}, ■ 0.1 mg mL^{-1}, ● 0.5 mg mL^{-1}, ∗ 1 mg mL^{-1}, ◆ 2 mg mL^{-1}) and evolution of different *P. putida* subpopulation during SA removal with TiO_2-NPs concentration of 0 mg mL^{-1} (B) 0.1 mg mL^{-1} (C), 0.5 mg mL^{-1} (D), 1 mg mL^{-1} (E) and 2 mg mL^{-1} (F). Subpopulation of VBNC cells, ▭ viable cells ▭ and dead cells ■ are plotted as percentage of the total cells counts on the principal y-axis. Metabolically active (∗), viable cells (■), dead cells (●) and damaged cells (▲) are expressed as cells mL^{-1} on the secondary y-axis. In all cases: Initial SA concentration of 500 mg L^{-1}, 250 rpm, 30 °C, *P. putida* inoculum of 10^7 CFU mL^{-1}, 100 mL in 500 mL Erlenmeyer flasks.

bacterium maintained its level of activity.

FSC and SSC were monitored during all SA removal time; both parameters increased with TiO_2 concentration and remained constant with time as in the case of GM (data no shown).

3.2. Segregated kinetic model: proposal and discussion

In order to quantify the SA removal of VBNC cells, experimental data for cell subpopulations and SA uptake were fitted to a segregated kinetic model (Quirós et al., 2007, 2009). For this model, the following assumptions were made:

- The total biomass, formed by viable (C_V), viable but non-culturable plus damaged cells (C_N) and dead cells (C_D), were expressed as bacterial concentrations (g L^{-1}), using the corresponding calibration curves determined previously (dry weight (g L^{-1}) = $8.17 \cdot 10^{-10}$ cells concentration (cells mL^{-1}).
- Viable cells are the cell subpopulation which shows the ability to grow on plates.
- Both viable and non-culturable fractions can lose their integrity, which results in the cellular death. VBNC cells are either not able to recover their "culturability".
- The SA removal was conducted by C_V and C_N

Taking into account the following considerations, the segregated model showed in Fig. 4a can be proposed. Based on this scheme, Equations (1)–(6) can easily be obtained, where r_1 and r_5 are the cell growth rates of viable and VBNC cells, r_2 is the transformation rate from viable to VBNC state, r_3 and r_4 are cell death rates of viable and VBNC cells, τ' and τ'' are the inverses of viable

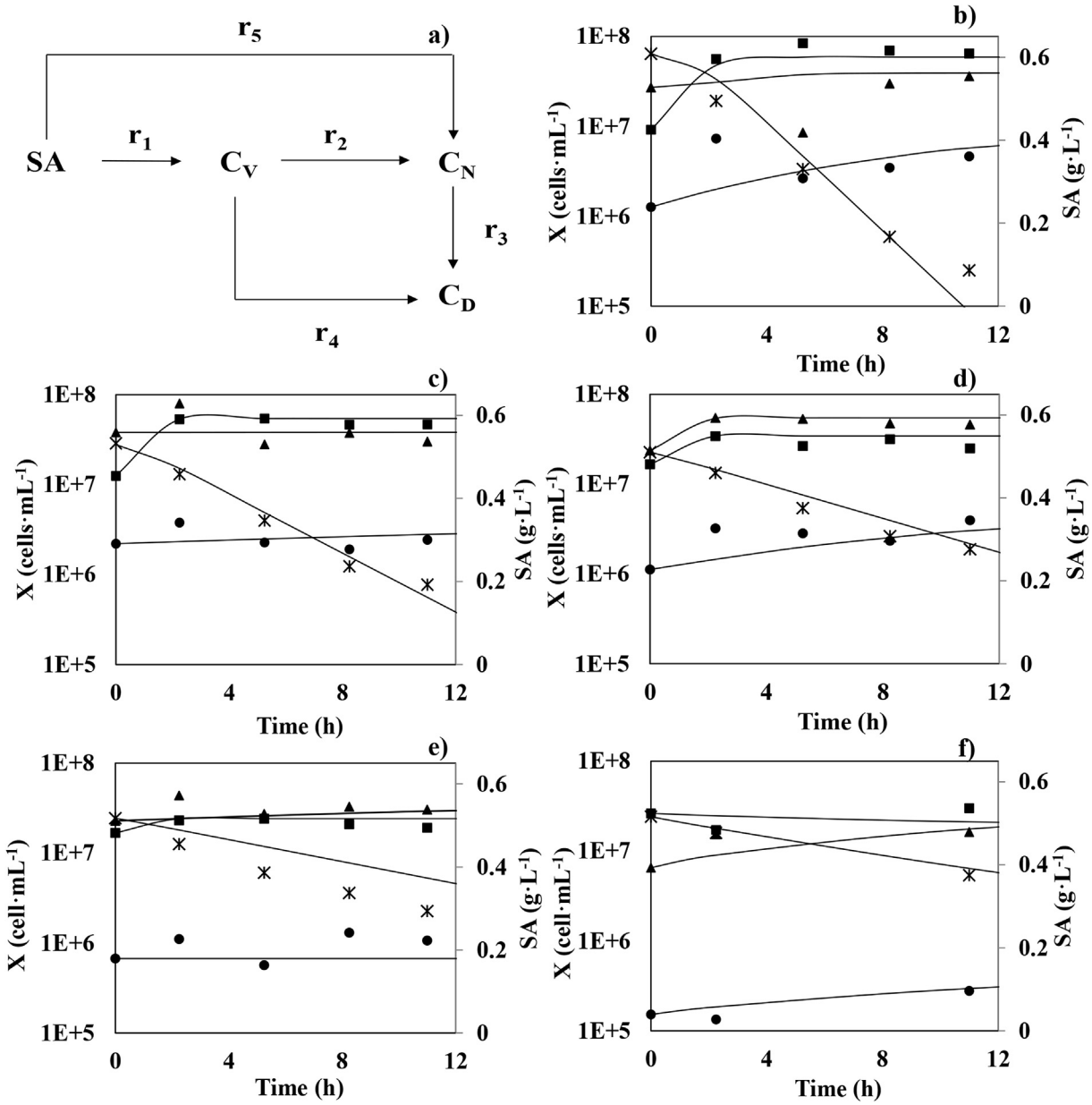

Fig. 4. Segregated kinetic model proposed (a) and evolution of VBNC (▲), viable (■) and dead cells (●) and SA concentration (∗) during the growth of *P. putida* in a SIW and in presence of different concentrations of TiO_2-NPs 0 mg mL^{-1} (b) 0.1 mg mL^{-1} (c), 0.5 mg mL^{-1} (d), 1 mg mL^{-1} (e) and 2 mg mL^{-1} (f). In all the cases: Initial SA concentration of 500 mg L^{-1}, 250 rpm, 30 °C, *P. putida* inoculum of 10^7 CFU mL^{-1}, 100 mL in 500 mL Erlenmeyer flask.

and VBNC cell concentrations in stationary phase, and q_V and q_N are the specific SA uptake rates for viable and VBNC subpopulations, respectively.

$$r_1 = k_1 \cdot C_V \cdot (1 - \tau' \cdot C_V) \quad (1)$$

$$r_2 = k_2 \cdot C_V \quad (2)$$

$$r_3 = k_3 \cdot C_N \quad (3)$$

$$r_4 = k_4 \cdot C_V \quad (4)$$

$$r_5 = k_5 \cdot C_N \cdot \left(1 - \tau'' \cdot C_N\right) \quad (5)$$

$$-\frac{dSA}{dt} = q_V \cdot C_V + q_N \cdot C_N \quad (6)$$

Equations (1)–(6) were fitted to experimental data from cell counting by flow cytometry and plate counting using *MicroMath Scientist® version 2.0*. Fig. 4 shows experimental and predicted data for *P. putida* growth curves and SA uptake with different concentrations of TiO_2-NPs. The value of the different kinetic parameters calculated for the proposed segregated kinetic model are collected in Table 1.

The model considering the growth of both viable and VBNC subpopulations provided a proper description of bacterial

Table 1
Kinetics parameters obtained for the segregated kinetic model proposed for *P. putida* growth and salicylic acid consumption in presence of TiO_2-NPs concentrations ranging from 0 to 2 mg mL^{-1}.

TiO_2 (mg mL^{-1})	k_1 (h^{-1})	k_2 (h^{-1})	k_3 (h^{-1})	k_4 (h^{-1})	k_5 (h^{-1})	q_V gSA (h gC_V)$^{-1}$	q_N gSA (h gC_N)$^{-1}$	τ' (L g^{-1})	τ'' (L g^{-1})
0	0.047	0.009	$1.2\cdot10^{-6}$	$3.0\cdot10^{-7}$	0.027	0.95	0.070	14.5	11.8
0.1	0.045	0.035	$1.4\cdot10^{-6}$	$1.9\cdot10^{-7}$	0.049	0.8	0.065	22.5	15.3
0.5	0.037	0.043	$3.3\cdot10^{-6}$	$3.3\cdot10^{-7}$	0.052	0.73	0.061	35.7	22.4
1	0.031	0.054	$3.7\cdot10^{-6}$	$1.4\cdot10^{-7}$	0.069	0.67	0.054	50.6	28.0
2	0.041	0.032	$1.5\cdot10^{-6}$	$1.6\cdot10^{-7}$	0.025	0.6	0.045	40.9	25.7

populations, as well as carbon source uptake (Quirós et al., 2007).

As can be seen in Table 1, the growth kinetic constant for viable bacteria is higher than their transformation kinetic constant into non-culturable cells ($k_1 > k_2$) for the experiment without nanoparticles. In addition, these non-culturable bacteria are mainly generated from division of others non-culturable bacteria, instead of from the viable cells which has loosen their capacity to growth in plate ($k_5 > k_2$). The increase in the TiO_2-NPs concentration leads to higher values of k_5 and k_2 and lower values of k_1. These findings indicate that nanoparticles had a negative effect on the viable subpopulation growth (k_1) but a positive effect on the viable but non-culturable cells formation rate, increasing their generation beginning from either the own multiplication (k_5) or the culturability loss of viable cells (k_2). In addition, when are compared with the others constants, the values of k_3 and k_4 were no significant, indicating that death reactions were a lot slower than the rest of the proposed ones.

Finally, q_V and q_N values can be used to discuss the effects of TiO_2-NPs on the *P. putida* capacity to degrade SA. In absence of nanoparticles, the specific degradative capacity for the viable subpopulation was far higher than for the viable but non-culturable subpopulation. This suggests that the entrance of viable cells into the VBNC state can be also accompanied by a reduction in substrate transport and metabolic activity levels in order to minimize cellular energetic requirements (Bogosian and Bourneuf, 2001; Quirós et al., 2007, 2009). A similar behaviour has been observed for non-culturable *Lactobacillus higardii* in response to SO_2 presence (Quirós et al., 2009). The presence of TiO_2-NPs reduced appreciably specific SA uptake rates for viable and VBNC subpopulations. So, qv in the SIW ranged from 0.9 gSA (h gCV)$^{-1}$ in absence of nanoparticles to 0.6 gSA (h gCV)$^{-1}$ when the concentration was 2 mg mL^{-1}. Interestingly, the q_V/q_N ratio kept approximately constant, at a value close to 12.7, suggesting that the inhibitory effect of the nanoparticles is similar for both subpopulations.

4. Conclusions

In this work, FC technique allows the study of the TiO_2-NPs effect on the physiological state of the *P. putida*. The increase of TiO_2-NPs concentrations meant a decrease of the total cell concentrations in the medium, a change in the physiological state of the bacteria was also observed since viable cells (CFU mL^{-1}) became VBNC cells. However, significant increases in the damaged or dead cells concentration were not produced. Using FC technique, FSC and SSC parameters were also measured, obtaining, in this case, an increase of both parameters with higher TiO_2-NPs concentration, which is due to NPs uptake in bacteria.

The viable cells transformation into VBNC cells affects the SA biodegradation since the metabolic capacity of VBNC cells is generally lower than that of viable cells. Finally, a segregated model including viable, VBNC and dead bacteria was fitted to the experimental data obtaining the growth and removal constants for each subpopulation.

Acknowledgements

R.G. Combarros wishes to express gratitude for a research grant from the Government of the Principality of Asturias (Severo Ochoa Programme).

Appendix A. Supplementary data

Supplementary data related to this article can be found at http://dx.doi.org/10.1016/j.watres.2015.12.040.

References

Amor, K.B., Breeuwer, P., Verbaarschot, P., Rombouts, F.M., Akkermans, A.D.L., De Vos, W.M., Abee, T., 2002. Multiparametric flow cytometry and cell sorting for the assessment of viable, injured, and dead bifidobacterium cells during bile salt stress. Appl. Environ. Microbiol. 68, 5209–5216. http://dx.doi.org/10.1128/aem.68.11.5209-5216.2002.

Anil, K., Zaidi, M.G.H., 2010. Implications of SPION and NBT nanoparticles upon in vitro and in situ biodegradation of LDPE film. J. Microbiol. Biotechnol. 20 http://dx.doi.org/10.4014/jmb.0912.12026.

Besinis, A., De Peralta, T., Handy, R.D., 2014. The antibacterial effects of silver, titanium dioxide and silica dioxide nanoparticles compared to the dental disinfectant chlorhexidine on *Streptococcus mutans* using a suite of bioassays. Nanotoxicology 8, 1–16. http://dx.doi.org/10.3109/17435390.2012.742935.

Bogosian, G., Bourneuf, E.V., 2001. A matter of bacterial life and death EMBO. Reports 2, 770–774. http://dx.doi.org/10.1093/embo-reports/kve182.

Bonnefond, A., González, E., Asua, J.M., Leiza, J.R., Kiwi, J., Pulgarin, C., Rtimi, S., 2015. New evidence for hybrid acrylic/TiO_2 films inducing bacterial inactivation under low intensity simulated sunlight. Colloids Surfaces B Biointerfaces 135, 1–7. http://dx.doi.org/10.1016/j.colsurfb.2015.07.034.

Collado, S., Rosas, I., González, E., Gutierrez-Lavin, A., Diaz, M., 2014. *Pseudomonas putida* response in membrane bioreactors under salicylic acid-induced stress conditions. J. Hazard. Mater. 267, 9–16. http://dx.doi.org/10.1016/j.jhazmat.2013.12.034.

Combarros, R.G., Collado, S., Laca, A., Díaz, M., 2015a. Conditions and mechanisms in thiocyanate biodegradation. J. Residuals Sci. Technol. 12.

Combarros, R.G., Collado, S., Laca, A., Díaz, M., 2015b. Understanding the simultaneous biodegradation of thiocyanate and salicylic acid by *Paracoccus thiocyanatus* and *Pseudomonas putida*. Int. J. Environ. Sci. Technol. http://dx.doi.org/10.1007/s13762-13015-10906-y (in press), ISSN: 1735-1472.

Combarros, R.G., Rosas, I., Lavín, A.G., Rendueles, M., Díaz, M., 2014. Influence of biofilm on activated carbon on the adsorption and biodegradation of salicylic acid in wastewater. Water Air Soil Pollut. 225, 1–12. http://dx.doi.org/10.1007/s11270-013-1858-9.

Cho, M., Chung, H., Choi, W., Yoon, J., 2004. Linear correlation between inactivation of *E. coli* and OH radical concentration in TiO_2 photocatalytic disinfection. Water Res. 38, 1069–1077. http://dx.doi.org/10.1016/j.watres.2003.10.029.

Díaz, M., Herrero, M., García, L.A., Quirós, C., 2010. Application of flow cytometry to industrial microbial bioprocesses. Biochem. Eng. J. 48, 385–407. http://dx.doi.org/10.1016/j.bej.2009.07.013.

Erdural, B., Bolukbasi, U., Karakas, G., 2014. Photocatalytic antibacterial activity of TiO_2–SiO_2 thin films: the effect of composition on cell adhesion and antibacterial activity. J. Photochem. Photobiol. A Chem. 283, 29–37. http://dx.doi.org/10.1016/j.jphotochem.2014.03.016.

Fu, G., Vary, P.S., Lin, C.-T., 2005. Anatase TiO_2 nanocomposites for antimicrobial coatings. J. Phys. Chem. B 109, 8889–8898. http://dx.doi.org/10.1021/jp0502196.

Gelover, S., Gómez, L.A., Reyes, K., Teresa Leal, M., 2006. A practical demonstration of water disinfection using TiO_2 films and sunlight. Water Res. 40, 3274–3280. http://dx.doi.org/10.1016/j.watres.2006.07.006.

Ghosh, M., J, M., Sinha, S., Chakraborty, A., Mallick, S.K., Bandyopadhyay, M., Mukherjee, A., 2012. In vitro and in vivo genotoxicity of silver nanoparticles. Mutat. Research/Genetic Toxicol. Environ. Mutagen. 749, 60–69. http://dx.doi.org/10.1016/j.mrgentox.2012.08.007.

Giraffa, G., 2004. Studying the dynamics of microbial populations during food fermentation. FEMS Microbiol. Rev. 28, 251–260. http://dx.doi.org/10.1016/

j.femsre.2003.10.005.
Hammes, F., Berney, M., Wang, Y., Vital, M., Köster, O., Egli, T., 2008. Flow-cytometric total bacterial cell counts as a descriptive microbiological parameter for drinking water treatment processes. Water Res. 42, 269–277. http://dx.doi.org/10.1016/j.watres.2007.07.009.
Hsu, Y.-C., Yang, H.-C., Chen, J.-H., 2004. The enhancement of the biodegradability of phenolic solution using preozonation based on high ozone utilization. Chemosphere 56, 149–158. http://dx.doi.org/10.1016/j.chemosphere.2004.02.011.
Ju-Nam, Y., Lead, J.R., 2008. Manufactured nanoparticles: an overview of their chemistry, interactions and potential environmental implications. Sci. Total Environ. 400, 396–414. http://dx.doi.org/10.1016/j.scitotenv.2008.06.042.
Kapri, A., Zaidi, M.G.H., Goel, R., 2009. Nanobarium titanate as supplement to accelerate plastic waste biodegradation by indigenous bacterial consortia. AIP Conf. Proc. 1147, 469–474. http://dx.doi.org/10.1063/1.3183475.
Kuang, Y., Zhou, Y., Chen, Z., Megharaj, M., Naidu, R., 2013. Impact of Fe and Ni/Fe nanoparticles on biodegradation of phenol by the strain Bacillus fusiformis (BFN) at various pH values. Bioresour. Technol. 136, 588–594. http://dx.doi.org/10.1016/j.biortech.2013.03.018.
Kumar, A., Pandey, A.K., Singh, S.S., Shanker, R., Dhawan, A., 2011. A flow cytometric method to assess nanoparticle uptake in bacteria. Cytom. Part A 79A, 707–712. http://dx.doi.org/10.1002/cyto.a.21085.
Le, T., Murugesan, K., Kim, E.-J., Chang, Y.-S., 2014. Effects of inorganic nanoparticles on viability and catabolic activities of Agrobacterium sp. PH-08 during biodegradation of dibenzofuran. Biodegradation 25, 655–668. http://dx.doi.org/10.1007/s10532-014-9689-y.
Li, B., Huang, W., Zhang, C., Feng, S., Zhang, Z., Lei, Z., Sugiura, N., 2015. Effect of TiO_2 nanoparticles on aerobic granulation of algal–bacterial symbiosis system and nutrients removal from synthetic wastewater. Bioresour. Technol. 187, 214–220. http://dx.doi.org/10.1016/j.biortech.2015.03.118.
Li, D., Cui, F., Zhao, Z., Liu, D., Xu, Y., Li, H., Yang, X., 2014. The impact of titanium dioxide nanoparticles on biological nitrogen removal from wastewater and bacterial community shifts in activated sludge. Biodegradation 25, 167–177. http://dx.doi.org/10.1007/s10532-013-9648-z.
Neal, A., 2008. What can be inferred from bacterium–nanoparticle interactions about the potential consequences of environmental exposure to nanoparticles? Ecotoxicology 17, 362–371. http://dx.doi.org/10.1007/s10646-008-0217-x.
Quirós, C., Herrero, M., García, L.A., Díaz, M., 2007. Application of flow cytometry to segregated kinetic modeling based on the physiological states of microorganisms. Appl. Environ. Microbiol. 73, 3993–4000. http://dx.doi.org/10.1128/AEM.00171-07.
Quirós, C., Herrero, M., García, L.A., Díaz, M., 2009. Quantitative approach to determining the contribution of viable-but-nonculturable subpopulations to malolactic fermentation processes. Appl. Environ. Microbiol. 75, 2977–2981. http://dx.doi.org/10.1128/AEM.01707-08.
Rawat, J., Rana, S., Srivastava, R., Misra, R.D.K., 2007. Antimicrobial activity of composite nanoparticles consisting of titania photocatalytic shell and nickel ferrite magnetic core. Mater. Sci. Eng. C 27, 540–545. http://dx.doi.org/10.1016/j.msec.2006.05.021.
Rincón, A.-G., Pulgarin, C., 2007. Absence of *E. coli* regrowth after Fe3+ and TiO_2 solar photoassisted disinfection of water in CPC solar photoreactor. Catal. Today 124, 204–214. http://dx.doi.org/10.1016/j.cattod.2007.03.039.
Toduka, Y., Toyooka, T., Ibuki, Y., 2012. Flow cytometric evaluation of nanoparticles using side-scattered light and reactive oxygen species-mediated fluorescence–correlation with genotoxicity. Environ. Sci. Technol. 46, 7629–7636. http://dx.doi.org/10.1021/es300433x.
Ziglio, G., Andreottola, G., Barbesti, S., Boschetti, G., Bruni, L., Foladori, P., Villa, R., 2002. Assessment of activated sludge viability with flow cytometry. Water Res. 36, 460–468. http://dx.doi.org/10.1016/S0043-1354(01)00228-7.
Zucker, R.M., Massaro, E.J., Sanders, K.M., Degn, L.L., Boyes, W.K., 2010. Detection of TiO_2 nanoparticles in cells by flow cytometry. Cytom. Part A 77A, 677–685. http://dx.doi.org/10.1002/cyto.a.20927.